# Real-Time Operational Assessment Of A Hybrid AC-DC Grid With Wind Integration Under Normal And Faulted Conditions

Trinh Trung Hieu*
The University of Danang - University of Science and Technology, Danang, Vietnam
* Corresponding author: tthieu@dut.udn.vn

Tran Hoang Minh
The University of Danang - University of Science and Technology, Danang, Vietnam
Hoangminhid14@gmail.com

Bui Hieu Thanh
The University of Danang - University of Science and Technology, Danang, Vietnam
bhthanh25dut@gmail.com

Tran Kim Nhat
Center for Environmental Intelligence, VinUniversity, Ha Noi, Vietnam
nhat.tk@vinuni.edu.vn

Tran Anh Tuan
The University of Danang - University of Science and Technology, Danang, Vietnam
tatuan@dut.udn.vn

***Abstract*—The increasing penetration of offshore wind generation introduces significant operational challenges due to its stochastic and intermittent nature. The rapid growth of renewable energy penetration, along with the increasing requirement for efficient long-distance bulk power transfer, has driven strong interest in hybrid AC-DC power grid architectures. This paper investigates the application of a multi-terminal high-voltage direct current (MTDC) system embedded in a hybrid AC-DC grid for assessing real-time operating behavior, with the objective of improving overall system stability. The study is carried out by implementing a hybrid grid model derived from the CIGRE B4.57 benchmark in DIgSILENT PowerFactory. Wind generation and load demand are modeled as time-varying signals. Both steady-state and time-domain simulations are performed under normal operation and contingency conditions, including an AC line outage three-phase fault. The results show that the MTDC grid maintains bus voltages more effectively than a conventional AC network. Although the power flows on the transmission lines fluctuate as the generation and load vary over time, they remain within acceptable operating limits. In particular, when temporary faults occur on both the DC and AC lines, the system voltage experiences only a short-term deviation and is quickly restored to a stable post-fault condition. These findings indicate that the MTDC-based grid not only enhances power transfer flexibility but also significantly improves voltage stability and overall system operational reliability.**

**Keywords- hybrid AC-DC grid; MTDC; wind power; quasi-dynamic simulation**

## I. Introduction

The global transition toward sustainable energy systems has led to unprecedented growth in renewable energy integration, particularly offshore wind power. In 2023, global additions to renewable power capacity increased by approximately 36% to reach 473 GW [1]. However, integrating high shares of renewable energy sources into utility-scale power systems remains a significant challenge due to their inherent variability [2].

Wind power variability introduces operational challenges including voltage fluctuation, reactive power imbalance, and frequency deviations, especially when integrated into weak networks [3], [4]. Wang et al. demonstrated that the influence of wind variability on system dynamics strongly depends on operating conditions and instantaneous penetration level [5].

Voltage source converter-based high voltage direct current (VSC-HVDC) transmission has emerged as a transformative solution for offshore wind integration. VSC-HVDC offers significant advantages including active-power control, reactive-power support, fast disturbance response, and black-start capability [6], [7]. As the scale of offshore wind generation increases, multi-terminal HVDC (MTDC) systems have emerged as a viable solution for integrating large-scale offshore wind farms [8], [9].

Research has shown that voltage droop control is highly preferred in MTDC systems because it enables decentralized power-sharing without extensive communication infrastructure [10], [11]. Pan et al. presented a design-oriented transient stability analysis of grid-forming VSCs, revealing that droop control with low-pass filters can be destabilized even if equilibrium points exist [12]. Wang et al. proposed a distributed cooperative control strategy for VSC-MTDC systems that achieves better frequency support without large DC voltage deviation [13].

Several research gaps remain in this field. First, most existing studies focus on either steady-state analysis or isolated transient scenarios, lacking a unified framework combining quasi-dynamic daily operation assessment with transient fault analysis. Second, few studies provide comprehensive validation using standardized benchmark systems with time-varying renewable generation profiles. Third, there is limited quantitative analysis of system behavior under realistic operating conditions.

To address these gaps, this paper presents a comprehensive operational assessment framework with the following contributions:

1. A unified simulation framework integrating steady-state power flow, 24-hour quasi-dynamic simulation, and RMS-based transient analysis based on the CIGRE B4.57 benchmark system
2. Implementation of realistic wind generation and load demand profiles with 5-minute resolution to capture daily operational variability.
3. Systematic evaluation of system response under multiple fault scenarios with quantitative performance metrics and recovery time analysis.

## II. SYSTEM MODEL AND SIMULATION FRAMEWORK

This section describes the hybrid AC-DC test system and simulation framework. The model is developed from the CIGRE B4.57 benchmark system and implemented in DIgSILENT PowerFactory [14], which has been widely used for hybrid AC-DC grid studies [15]–[17]. To represent renewable integration, two 300 MW offshore wind farms are added to the network through dedicated transformers. The developed model, including AC-DC subsystems, converters, transformers, transmission lines, external grids, conventional generators, and wind farms, is used to assess system performance under normal and disturbed operating conditions, as shown in Fig. 1.

The wind power and load demand profiles used in this study are shown in Fig. 2 and Fig. 3, respectively. These time-varying profiles are applied to represent realistic operating conditions instead of assuming constant generation and load values.

The representative source groups and their generation settings are summarized in Table I, while the transformer data are presented in Table II. The electrical parameters of the AC and DC line types are listed in Table III. In addition, the main parameters of the DC/DC converters and the ratings of the AC-DC converters are detailed in Tables IV and V.

TABLE I REPRESENTATIVE SOURCE AND GENERATION SETTINGS

| Source group | V (kV) | Ssc (GVA) | Control / setpoint |
|---|---|---|---|
| Ext_Grid_A0/ Ext_Grid_B0 | 380 | 30 | V = 1.00 p.u.; φ = 0° |
| G-A1 | 380 | 30 | P = 2000 MW; Q = 0 MVAr |
| G-B1 / G-B2 / G-B3 | 380 | 30 | P = 1000 MW ; Q = 0 MVAr |
| G-C1 / G-C2 / G-F1 | 145 | 8 | P = 500 MW ; Q = 0 MVAr |
| G-D1 | 145 | 8 | P = 1000 MW; Q = 0 MVAr |

*email: tthieu@dut.udn.vn

TABLE II REPRESENTATIVE TRANSFORMER DATA

| Transformer group | HV/LV (kV) | Rated power (MVA) | X / R (p.u.) | Connection |
|---|---|---|---|---|
| Tr_Cm_A1/ Tr_Cm_B2 | 380/220 | 800 | 0.18 / 0.006 | YNd0 |
| Tr_Cb-A1 pos,neg/ Tr_Cb-B1 pos,neg/ Tr_Cm_B3 | 380/220 | 1200 | 0.18 / 0.006 | YNd0 |
| Tr_Cm_C1/ Tr_Cm_E1/ Tr_Cm_F1/ Tr_Cb-D1 pos,neg | 220/145 | 800 | 0.18 / 0.006 | YNd0 |
| Tr_Cb-C2 pos,neg | 220/145 | 400 | 0.18 / 0.006 | YNd0 |

TABLE III LINE TYPES

| Line type | R [Ω/km] | L [mH/km] | C [μF/km] | G [μS/km] | Max. current [A] |
|---|---|---|---|---|---|
| DC OHL +/- 400kV | 0.0114 | 0.9356 | 0.0123 | - | 3500 |
| DC OHL +/- 200kV | 0.0133 | 0.8273 | 0.0139 | - | 3000 |
| DC cable +/- 400kV | 0.011 | 2.615 | 0.1908 | 0.048 | 2265 |
| DC cable +/- 200kV | 0.011 | 2.615 | 0.2185 | 0.055 | 1962 |
| AC cable 145kV | 0.0843 | 0.2526 | 0.1837 | 0.041 | 715 |
| AC OHL 380kV | 0.0200 | 0.8532 | 0.0135 | - | 3555 |

TABLE IV DC/DC CONVERTERS

| DC/DC Converter | Alpha U2/U1 | Rated Current in A |
|---|---|---|
| Cd-B1 pos/ Cd-B1 neg | 1 | 5000 |
| Cd-E1 pos | 0.5 | 5000 |
| Cd-E1 neg | 2 | 5000 |

TABLE V AC-DC CONVERTERS

| AC-DC Converter | Ur AC (kV) | Ur DC (kV) | Rated Power (MVA) | Copper Losses (kW) | Resistive Loss Factor (mΩ) |
|---|---|---|---|---|---|
| Cm-A1/ Cm-B2/ Cb-B2_pos/ Cb-B2_neg/ Cm-C1/ Cb-D1_pos/ Cb-D1_neg/ Cm-F1. | 220 | 400 | 800 | 2400 | 242 |
| Cb-A1_pos/ Cb-A1_neg/ Cb-B1_pos/ Cb-B1_neg/ Cm-B3 | 220 | 400 | 1200 | 3600 | 161.3333 |
| Cb-C2_pos/ Cb-C2_neg | 220 | 400 | 400 | 1200 | 484 |
| Cm-E1 | 220 | 400 | 200 | 600 | 968 |

Three simulation scenarios are considered to evaluate system performance. Scenario 1 is a 24-hour quasi-dynamic simulation under varying wind generation and load demand. Scenario 2 examines the response of the DC subsystem to a short-circuit fault on a DC line, while Scenario 3 investigates the impact of a short-circuit fault on an AC line on power flow, voltage, and system stability.

https://doi.org/10.1051/e3sconf/202672302006

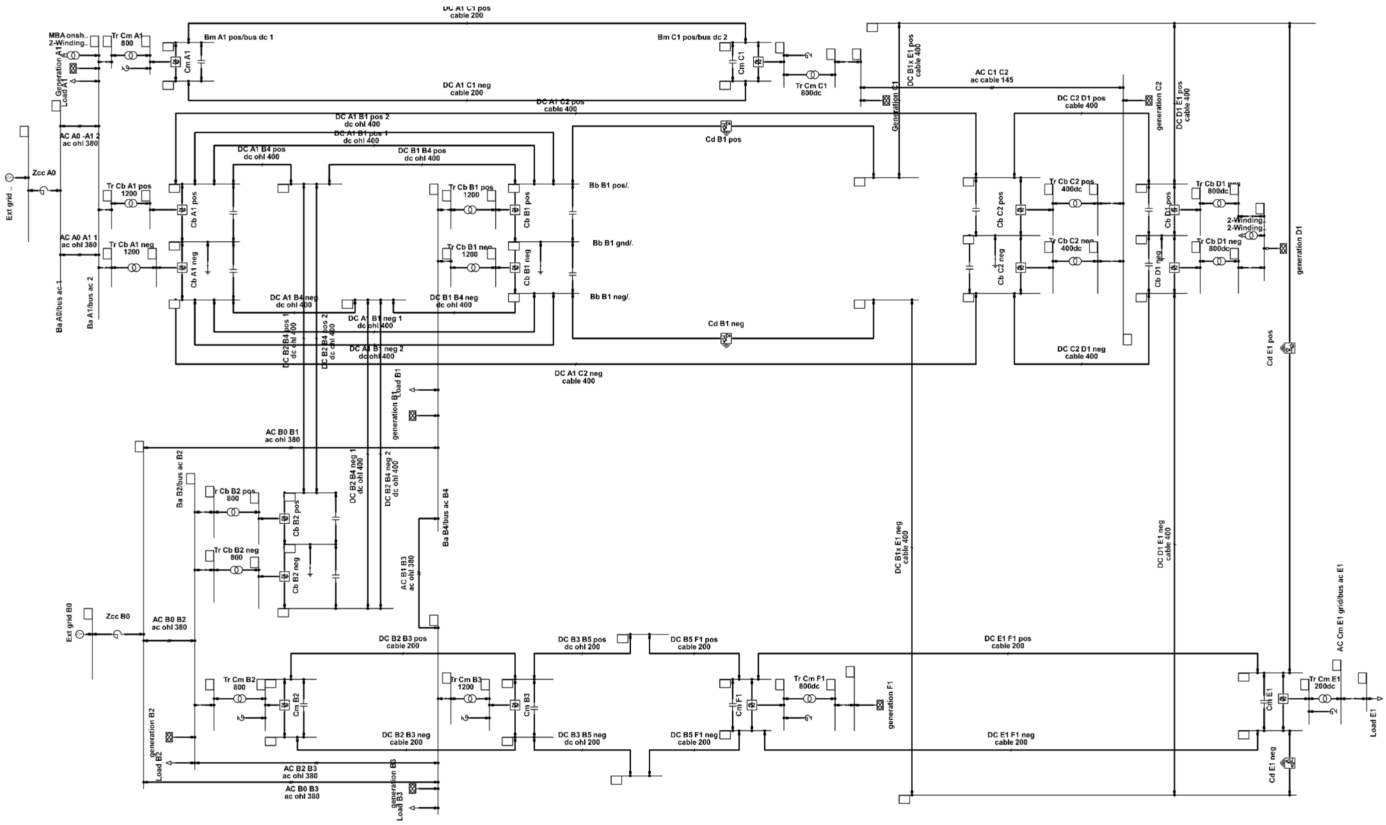

Fig. 1 OVERALL HYBRID AC-DC NETWORK LAYOUT USED FOR POWERFACTORY MODELING

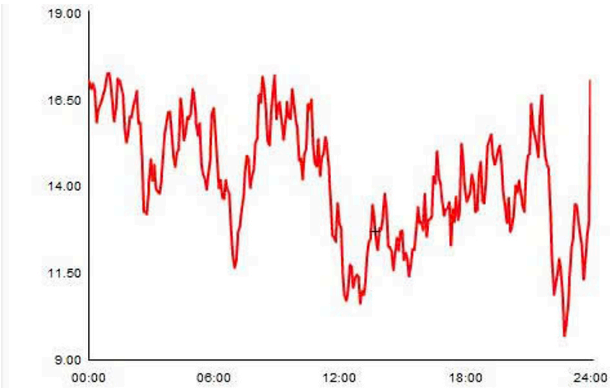


Fig. 2 24-HOUR WIND SPEED PROFILE

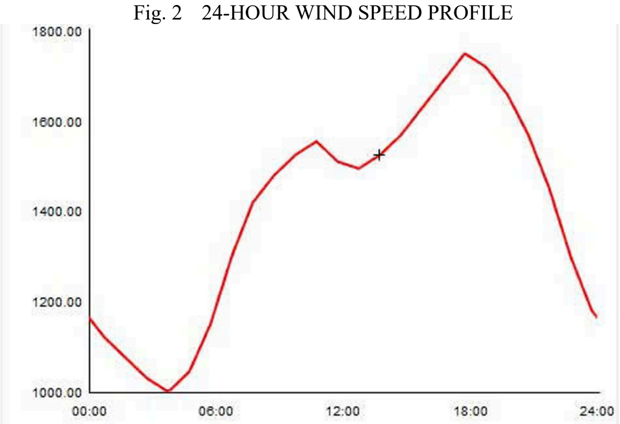


Fig. 3 24-HOUR LOAD DEMAND PROFILE

## III. RESULTS AND DISCUSSION

### *A.* Scenario 1: Quasi-dynamic 24-Hour Operation

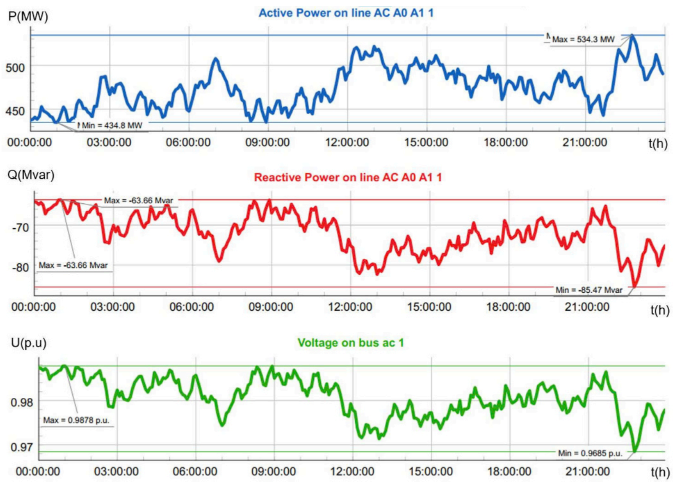


Fig. 4 QUASI-DYNAMIC 24-HOUR SIMULATION RESULTS

Fig. 4 presents the 24-hour quasi-dynamic response of the hybrid AC/DC grid under simultaneous variations in wind generation and load demand. The active power on line AC A0–A1 1 varies between 434.8 MW and 534.3 MW, following the daily change in net generation and system demand. The smooth variation of active power indicates that the monitored AC corridor can redistribute power continuously without abrupt power swings or sustained oscillations. This behavior confirms that the hybrid AC/DC structure can accommodate slow

 https://doi.org/10.1051/e3sconf/202672302006

variations in renewable generation while maintaining stable power transfer.

The reactive power on the same line remains negative throughout the simulation, ranging from −63.66 MVAr to −85.47 MVAr. This result indicates a consistent reactive-power exchange pattern along the monitored AC line under the adopted sign convention. The variation in reactive power is associated with the change in active-power transfer, line voltage drop, and the reactive-power requirement of the surrounding AC network. Therefore, the reactive-power profile reflects not only the loading condition of the line but also the voltage-support requirement of the AC subsystem during daily operation.

The voltage at Bus AC 1 is maintained within a narrow range from 0.9685 p.u. to 0.9878 p.u. Although the voltage is slightly below the nominal value, it remains above the typical lower operating limit of 0.95 p.u. during the entire simulation period. No progressive voltage decline or voltage instability is observed, even when wind generation and load demand vary over time. This demonstrates that the hybrid AC/DC grid provides sufficient voltage regulation capability under quasi-dynamic operating conditions. Overall, the results show that the studied system can absorb daily renewable and load variations while preserving acceptable voltage stability and secure power transfer. Similar voltage behavior is also observed at other monitored buses in the network. Similarly, comparable results can also be observed at the other buses in the network.

TABLE VI MAXIMUM AND MINIMUM BUS VOLTAGE VALUES UNDER 24-HOUR QUASI-DYNAMIC OPERATION

| Bus name | $U_{max}$ (p.u) | $U_{min}$ (p.u) |
|---|---|---|
| Bus ac 2 | 0.9907 | 0.9856 |
| Bus ac B2 | 1.0033 | 1.0027 |
| Bus ac B4 | 1.0002 | 1.0001 |
| Bus ac E1 | 0.9923 | 0.9920 |
| Bus dc 1 | 1.0000 | 1.0000 |

### B. Scenario 2: DC Line Short-Circuit Fault

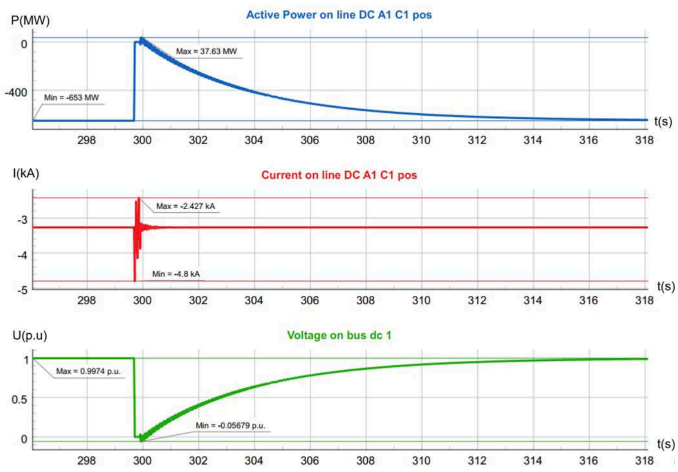


Fig. 5 TRANSIENT RESPONSE OF LINE DC A1–C1 POS AND DC BUS 1 UNDER A SHORT-CIRCUIT FAULT AT BUS DC 1

Fig. 5 presents the transient response of the DC subsystem when a short-circuit fault is applied at Bus DC 1. Before the fault, line DC A1–C1 pos transfers approximately −653 MW with a current of about −3.2 kA, while the DC voltage remains close to its nominal value at 0.9974 p.u. When the fault occurs at around 299.7 s, the DC voltage collapses sharply to about −0.05679 p.u., indicating a severe loss of voltage support at the faulted bus. The line current also experiences a transient excursion between −4.8 kA and −2.427 kA, which can be associated with the discharge of stored energy from the DC-link and line capacitances. Meanwhile, the active power undergoes a temporary reversal and reaches about 37.63 MW before gradually recovering. After fault clearance, the current settles faster than the DC voltage and active power, showing that the DC voltage control dynamics require more time to restore the operating point. Overall, the DC-side fault causes a severe but temporary disturbance, and the MTDC system can recover to a stable post-fault condition without prolonged instability.

### C. Scenario 3: AC Line Three-Phase Fault.

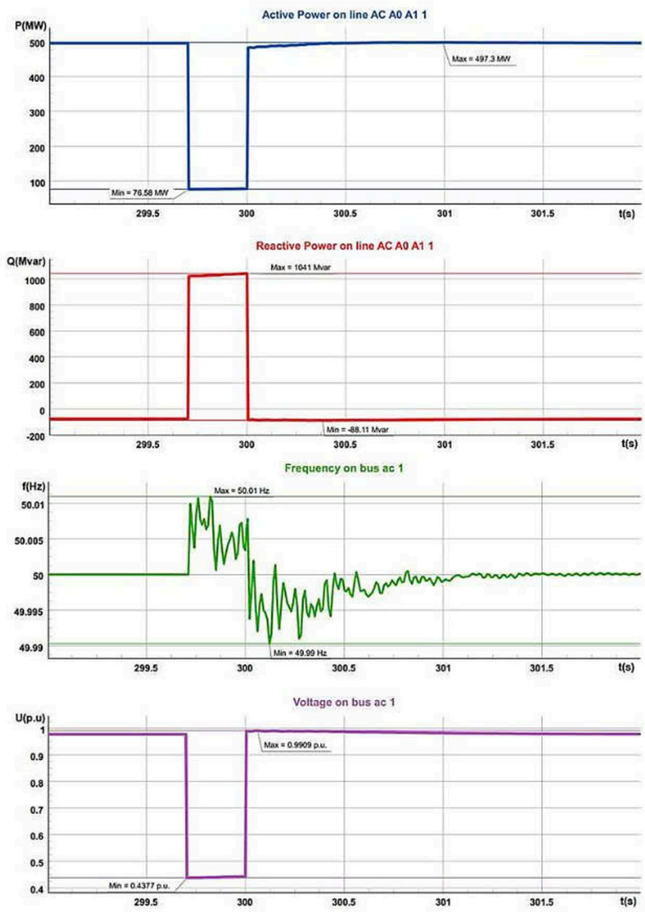


Fig. 6 ACTIVE POWER, REACTIVE POWER, FREQUENCY, AND VOLTAGE RESPONSE UNDER A THREE-PHASE FAULT ON LINE AC A0 A1 1

Fig. 6 shows the dynamic response of the hybrid AC/DC grid when a three-phase short-circuit fault is applied on line AC A0–A1 1 at 299.7 s and cleared after 0.3 s. During the fault period, the active power on the faulted line decreases sharply from approximately 500 MW to 76.58 MW. This reduction is mainly caused by the severe voltage depression at the faulted area, which limits the active-power transfer capability of the AC corridor. From a power-system perspective, the fault significantly weakens the effective voltage difference supporting power transmission along the line, leading to a temporary collapse of active power transfer.

The reactive power response is more severe, increasing abruptly from the normal operating value of about −88.11 MVAr to a maximum of 1041 MVAr. This large reactive-power surge is a typical characteristic of a three-phase short-circuit fault, where the network requires substantial reactive current to support the depressed voltage and supply the fault current. Therefore, the reactive-power peak indicates that the AC subsystem experiences a strong voltage-support burden during the disturbance.

At Bus AC 1, the voltage drops rapidly to 0.4377 p.u., confirming a deep voltage sag caused by the three-phase fault. However, after fault clearance, the voltage recovers quickly to approximately 0.9909 p.u. without sustained oscillation. This response indicates that the system has sufficient post-fault voltage recovery capability and does not exhibit voltage instability after the disturbance is removed. In contrast, the frequency varies only within a narrow range from 49.99 Hz to 50.01 Hz. This limited frequency deviation suggests that the disturbance mainly affects local voltage and power-flow quantities, while the overall active-power balance of the system remains well maintained due to the short fault duration and the support of the interconnected grid/converter-controlled sources.

Overall, the AC-side fault produces a severe but localized disturbance, characterized by a sharp reduction in active power, a large reactive-power transient, and a deep voltage sag. Nevertheless, the rapid recovery of voltage, power flow, and frequency after fault clearance demonstrates the satisfactory dynamic stability and post-fault resilience of the MTDC-based hybrid AC/DC grid under a severe AC-side disturbance.

## IV. CONCLUSIONS

This paper presented an operational assessment of a multi-terminal hybrid AC-DC grid using a simulation framework implemented in DIgSILENT PowerFactory. Based on the CIGRE B4.57 benchmark system, the study incorporated wind power integration and evaluated system behavior under three representative scenarios, including a 24-hour quasi-dynamic operation, a DC-side short-circuit disturbance, and an AC-side three-phase fault. The results confirm that the proposed hybrid grid model is suitable for analyzing both time-varying operating conditions and transient fault responses in MTDC-based power systems.

Under the 24-hour quasi-dynamic scenario, the active and reactive power on the monitored AC line varied continuously with changing wind generation and load demand, while bus voltage remained within a narrow and acceptable range. This indicates that the hybrid AC-DC structure can maintain satisfactory steady operating performance despite renewable intermittency. In the DC fault scenario, the monitored DC quantities exhibited sharp transient deviations immediately after the disturbance, especially in power, current, and DC voltage, but recovered progressively after fault clearance. Similarly, in the AC fault case, the faulted line experienced a severe temporary reduction in active power, a large increase in reactive power demand, and a deep voltage sag at the nearby AC bus, whereas the frequency deviation remained very limited and the system returned rapidly to a stable post-fault state.

Overall, the obtained results demonstrate that the studied MTDC-based hybrid grid has good dynamic resilience, effective post-fault recovery capability, and acceptable operational stability under both normal and disturbed conditions. These findings provide a useful technical basis for further studies on coordinated converter control, adaptive protection strategies, and enhanced operational optimization for future large-scale renewable-integrated AC-DC transmission systems.

## REFERENCES

[1] International Energy Agency, Renewables 2023: Analysis and forecast to 2028 (2023)

[2] H. Du, T.B. Hashfi, R. Prasad, P.P. Vergara, P. Palensky, A. Lekic, Optimal droop control strategy for coordinated voltage regulation and power sharing in hybrid AC-MTDC systems, Electric Power Systems Research 220, 109881 (2024).

[3] J.O. Petinrin, M. Shaaban, Impact of renewable generation on voltage control in distribution systems, Renewable and Sustainable Energy Reviews 65, 770 (2016).

[4] S.R. Abbas et al., Impact analysis of large-scale wind farms integration in weak transmission grid from technical perspectives, IEEE Access 8, 149750 (2020).

[5] Y. Wang, V. Silva, M. Lopez-Botet-Zulueta, Impact of high penetration of variable renewable generation on frequency dynamics in the continental Europe interconnected system, IET Renewable Power Generation 10, 10 (2016).

[6] A. Alassi, S. Bañales, O. Ellabban, G. Adam, C. MacIver, HVDC transmission: Technology review, market trends and future outlook, Renewable and Sustainable Energy Reviews 112, 530 (2019).

[7] C.H. Lin, Y.K. Wu, W.T. Huang, Overview of frequency-control technologies for a VSC-HVDC-integrated wind farm, IEEE Access 9, 97619 (2021).

[8] Y. Li, Z. Xu, Coordinated control of wind farms and MTDC grids for system frequency support, IEEE Transactions on Power Systems 32, 2632 (2017).

[9] A. Raza, A. Shakeel, A. Altalbe, T. O'Donnell, Optimal power flow and unified control strategy for multi-terminal HVDC systems, IEEE Access 7, 92642 (2019).

[10] T.K. Vrana, J. Beerten, R. Belmans, O.B. Fosso, A classification of DC node voltage control methods for HVDC grids, Electric Power Systems Research 103, 137 (2013).

[11] J. Beerten, R. Belmans, A comprehensive modeling framework for dynamic and steady state analysis of voltage droop control strategies in HVDC grids, International Journal of Electrical Power & Energy Systems 73, 691 (2015).

[12] D. Pan, X. Wang, F. Liu, R. Shi, Transient stability of voltage-source converters with grid-forming control: A design-oriented study, IEEE Journal of Emerging and Selected Topics in Power Electronics 8, 1019 (2020).

[13] W. Wang, Y. Li, Y. Cao, U. Häger, C. Rehtanz, A distributed cooperative control based on consensus protocol for VSC-MTDC systems, IEEE Transactions on Power Systems 36, 2877 (2021).

[14] CIGRÉ Working Groups B4-58 and B4-57, The CIGRÉ B4 DC grid test system, Electra 270, 10 (2013).

[15] J. Renedo, A.A. Ibrahim, B. Kazemtabrizi, A. García-Cerrada, L. Rouco, Q. Zhao, J. García-González, A simplified algorithm to solve optimal power flows in hybrid VSC-based AC/DC systems, International Journal of Electrical Power & Energy Systems 110, 781 (2019).

[16] J. Beerten, R. Belmans, Development of an open source power flow software for high voltage direct current grids and hybrid AC/DC systems: MatACDC, IET Generation, Transmission & Distribution 9, 966 (2015).

[17] A. Alvarez-Bustos, B. Kazemtabrizi, M. Shahbazi, E. Acha, Universal branch model for the solution of optimal power flows in hybrid AC-DC grids, International Journal of Electrical Power & Energy Systems 126, 106543 (2021).

- Spelling and grammatical errors throughout the manuscript should be carefully reviewed and corrected.
→ In response to the comment on spelling and grammatical errors, the manuscript has been carefully proofread and revised to correct issues related to spelling, grammar, and wording.
- All four subfigures in Figure 6 should be presented over the same time frame to help readers more easily observe the variation of the four parameters over time.
→ For Fig. 6, the results have been revised to be presented within the same time frame.
- Table formatting is not fully compliant with IEEE style.
→ The tables have been revised according to the IEEE formatting standards
- Figures lack detailed interpretation. Figures (Fig. 4–6) are referenced but not deeply analyzed.
→ In response to the comment that the simulation results lacked in-depth analysis, the Results and Discussion section has been revised by adding further technical analysis.